

PAPER • OPEN ACCESS

## Artificial Intelligence for rapid mapping of potential archaeological features using Bag of Visual Words based image classifier

To cite this article: Shairatul Akma Roslan *et al* 2024 *IOP Conf. Ser.: Earth Environ. Sci.* **1412** 012030

View the [article online](#) for updates and enhancements.

You may also like

- [On the LiDAR contribution for the archaeological and geomorphological study of a deserted medieval village in Southern Italy](#)  
Rosa Lasaponara, Rosa Coluzzi, Fabrizio T Gizzi *et al.*
- [Unravelling the role of iron and manganese oxides in colouring Late Antique glass by micro-XANES and micro-XRF spectroscopies](#)  
Francesca Gherardi, Clément Hole, Ewan Campbell *et al.*
- [Efficiency and quality raising in preventive archaeology: work in progress of the project ARCHEO 3.0](#)  
S Rescic, S Siano, R Manganelli Del Fà *et al.*



**ECS** The Electrochemical Society  
Advancing solid state & electrochemical science & technology

**247th ECS Meeting**  
Montréal, Canada  
May 18-22, 2025  
*Palais des Congrès de Montréal*

**Showcase your science!**

**Abstract submission deadline extended: December 20**

**ECS UNITED**

# Artificial Intelligence for rapid mapping of potential archaeological features using Bag of Visual Words based image classifier

Shairatul Akma Roslan<sup>1,2\*</sup>, Muhamad Sharifuddin Abd Rahim<sup>1</sup>, Fitri Yakub<sup>1</sup>,  
Yong Chee Kong<sup>2</sup>, and Norzailawati Mohd Noor<sup>3</sup>

<sup>1</sup>Malaysia Japan International Institute of Technology (MJIT), Jalan Sultan Yahya Petra, Universiti Teknologi Malaysia, 54100 Kuala Lumpur, Wilayah Persekutuan Kuala Lumpur.

<sup>2</sup>PLANMalaysia, Kementerian Perumahan dan Kerajaan Tempatan, Blok F5, Kompleks F, Presint 1, Pusat Pentadbiran Kerajaan Persekutuan, 62675 Putrajaya, Malaysia.

<sup>3</sup>Department of Urban & Regional Planning, Kuliyyah of Architecture & Environmental Design, International Islamic University Malaysia, Jln Gombak, 53100 Kuala Lumpur, Selangor.

\*E-mail: shairatulroslan@gmail.com

**Abstract.** Integrating Artificial Intelligence technological advancements in archaeology has revolutionised automated feature detection, presenting a novel perspective on archaeological feature recognition and image interpretation. This approach reduces costs associated with ground data collection and enhances the reliability and productivity of large-scale archaeological mapping. Consequently, this study aims to explore feature detection and matching techniques in archaeological detection using Artificial Intelligence and Scale-Invariant Feature Transform and Oriented Fast and Rotated Brief algorithms, which are frequently employed in image processing applications as a feature descriptor within the Bag-of-Visual-Words framework. The high-resolution multispectral satellite SPOT image maps potentially hidden archaeological features in Bujang Valley, Kedah, Malaysia. The expected outcome involves presenting a BoVW model capable of accurately detecting hidden archaeological features within the generated maps, thereby providing valuable insights into the extent and distribution of archaeological remnants in the targeted regions.

**Keywords:** Artificial Intelligence, SIFT, ORB, Bag of Visual Words, image analysis, Archaeology

## 1. Introduction

Along with the visual or image recognition approach in archaeology, the increasing number of studies in automatic or semi-automatic feature-detection techniques, such as Artificial Intelligence (AI) and Machine Learning methods, have developed great potential in automating feature detection to reveal



potential archaeological anomalies. Automated feature detection has a broad definition in different perspectives and contexts. Automated feature detection is image processing using computing extraction information methods and several computer vision algorithms. It can be performed successfully in image classification, segmentation, recognition, and prediction of objects in an image. It also allows archaeological features to be examined as individual objects within their broader spatial context.

Meanwhile, archaeological remote sensing using AI methods has seen a considerable upsurge in the last several years [1]. More efficient data collection and analysis can be achieved using AI methodologies and processes. For instance, integrating AI with remote sensing datasets at the most significant scale enables researchers to appropriately document human system dynamics, which in turn allows for extensive studies of settlement and mobility patterns, impacts of environmental change on human societies, ecological effects of anthropogenic land use, and other critical archaeological topics[2],[3]. According to [4], clear evidence of pattern recognition and image data will be practical, and the application of AI could potentially locate hidden archaeological feature properties. AI's improving predictive skills are leading to an upward trend in its use for archaeological prospection. Archaeology may greatly benefit from the comprehensive utilisation of data collecting to inform judgments regarding suitable ways for preserving and safeguarding archaeological artefacts.

Additionally, data collection can help determine the optimal location for excavation in a complex cultural environment. Based on recent archaeological investigations, a meticulously crafted model can yield reliable and precise outcomes, offering a probability estimate for recognising archaeological remains; however, this model does not aim to replace human specialists with automated detection [5]. They improve tasks such as scene understanding, object recognition, and navigation. More precisely, archaeologists can employ this method to identify probably concealed abnormalities related to archaeological findings. Several algorithms that can be utilised for image detection are the Harris Corner Detector, Scale-Invariant Feature Transform (SIFT), Speeded-Up Robust Features (SURF), Binary Robust Independent Elementary Features (BRIEF), Oriented FAST and Rotated BRIEF (ORB), and Features from Accelerated Segment Test (FAST).

Therefore, this paper introduces SIFT and ORB, Artificial Intelligence techniques for identifying and delineating within the Bujang Valley Archaeology Complex areas using SPOT-7, multispectral satellite imageries. SIFT and ORB are frequently employed in image processing applications as a feature descriptor within the Bag-of-Visual-Words (BOVW) framework. Mainly, SIFT is renowned for its ability to maintain scale and rotation invariance, which allows it to remain unaffected by variations in viewpoint and illumination. In feature extraction, SIFT is an effective technique to detect and describe image keypoints. These keypoints capture distinctive local features like edges, corners, and blobs. On the other hand, ORB provides a computationally efficient option demonstrating robust feature matching and localisation performance. Subsequently, the study findings are assessed, compared with prior field survey data, and deliberated along with the prevailing interpretations of the past study paths as a guideline and benchmark.

Integrating the high-resolution SPOT-7 dataset and the BoVW model can significantly enhance earlier technique utilisation and analysis in the Bujang Valley in the context of multispectral capabilities. Multispectral is well-known for identifying vegetation types, which can be crucial in distinguishing between natural formations and artificial structures because its high resolution can capture finer details, further improving the accuracy of site detection and analysis. Besides, it allows for rapid and extensive surveys of large areas, significantly reducing the time and labour involved. Furthermore, the BoVW model is advanced in capturing complex patterns characteristic of archaeological features through image processing methods. It is also efficiently allowable to classify and identify similar patterns in new images, aiding in discovering potential archaeological sites.

### 1.1 Study Background The Bujang Valley

The Bujang Valley, considered one of the most significant discoveries throughout recent historical events, has been selected as the site for testing the technique. [6] recognise the site as an important archaeological site in Malaysia. It is the original location of a kingdom known as "Kedah Tua" (ancient Kedah), dating back to the 6th century BCE. The Bujang Valley sites in Southern Kedah, Malaysia, have undergone extensive investigation, revealing significant amounts of undocumented evidence. Sungai Batu, Pengakalan Bujang, and Sungai Mas are prominent archaeological sites in Bujang Valley, known for their abundant archaeological artefacts. The evidence indicates that Bujang Valley is an ancient Southeast Asian site and is included in the prestigious UNESCO World Heritage list. In the past, it served as a prominent hub for international trade in black iron production. Figure 1 depicts the geographical geography and specific locations of the study areas within the Bujang Valley Archaeology Museum, situated in the Merbok region.



**Figure 1.** Key Map of Peninsular Malaysia and the spotted location of Bujang Valley, Kedah region (Source: Google Earth Pro).

### 1.2 Bujang Valley archaeological museum

Geographically, Bujang Valley lies in Merbok, South Kedah, which limits its territory to 144 square miles with the limitation of Bukit Choras in the north, the Muda River in the south, the Straits of Malacca in the eastern half, and the North-South Expressway in the West [7]. Topographically, Bujang Valley covers mountainous terrain, bald hills, river valleys, and beaches. **Figure 2** shows the Bujang Valley archaeological museum at the foot of Mount Jerai, the highest point in Bujang Valley, at an elevation of 1,300 meters above sea level [8]. According to an initial discovery by [9], Mount Jerai is formed up of symmetrical rock with various components and a layer of quartzite coating. Mount Jerai was previously a prominent navigational point for sailors crossing the Bay of Bengal to enter the Straits of Malacca [10]. It was also considered abundant in minerals and held spiritual significance as a dwelling place for a strong deity. Thus, because of these essential factors, Bujang Valley emerged as a strategic location for settlement and an important centre for commerce and industry [11]. Additionally,

it served as a temporary stop-over for sailors transiting to Arab or China in the east and to India and the Middle East in the west [12].

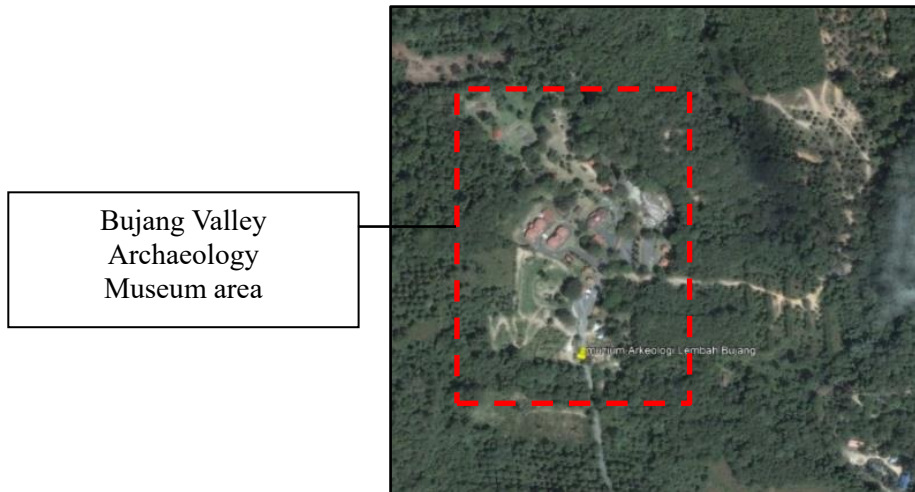


**Figure 2.** Location of the Bujang Valley Archaeological Museum region in the area of Mount Jerai.

## 2. Material and Techniques

Figure 3 illustrates a schematic workflow for the overall study flow. This schematic workflow chart outlines a process for handling and analysing image data, specifically for a multispectral SPOT-7 dataset of Bujang Valley, Kedah. The flow chart is divided into three main phases: Pre-Processing Phase, Keypoint Localisation, and Feature Matching and Pixel Range Evaluations. According to graph flow, the dataset utilised for this process is a multispectral SPOT-7 acquired in 2017 from Bujang Valley, Kedah. The study area of 400 km<sup>2</sup> is a primary dataset due to its high-resolution imagery and data availability from the previous research study. Overall, image processing has been analysed using Python in order to investigate and automatically identify potential archaeological monuments.



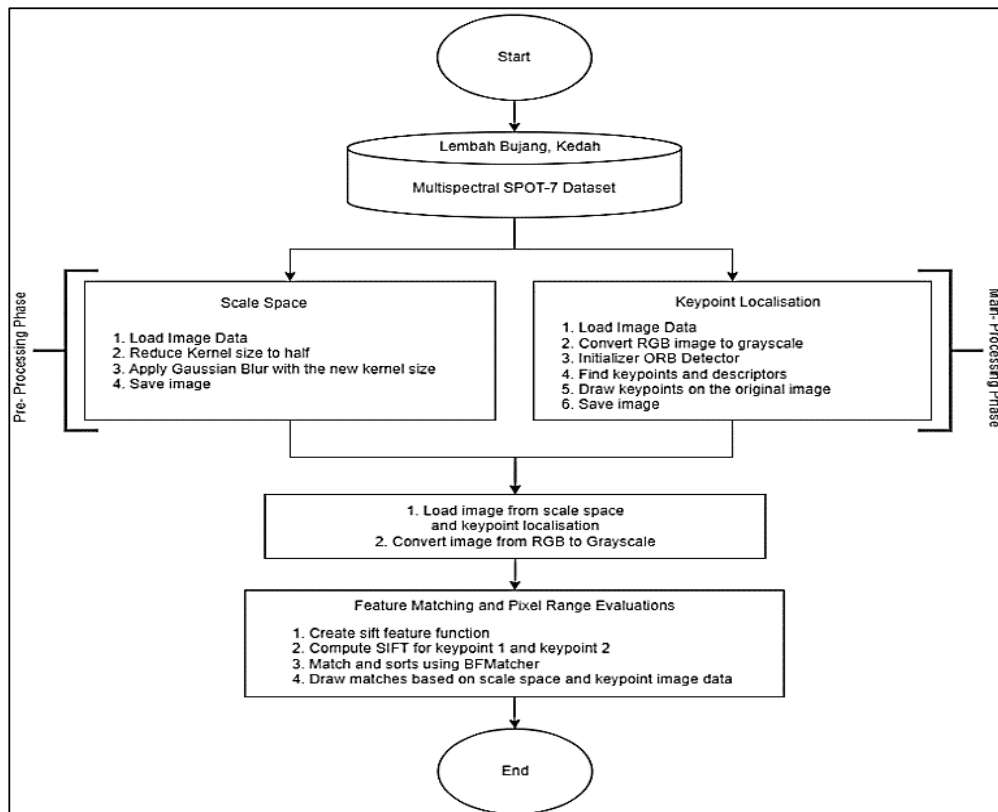


**Figure 3.** Schematic workflow for archaeological feature detection study using integration of remote sensing dataset and Artificial Intelligence; Oriented Fast and Rotated Brief and Scale-Invariant Feature Transform algorithms technique.

## 2.1 Data Availability

**2.1.1 Multispectral SPOT-7 Dataset.** The archaeological application of remote sensing satellite imaging has been dramatically extended in a decade. Satellite pour l'Observation de la Terre (SPOT) is a French word that means the satellite for observation of Earth. This particular satellite data image is suitable for archaeological detection as it provides high-resolution imagery and geospatial datasets. According to Table 1, SPOT 7 is multispectral imagery that incorporates four bands from the blue band (450nm – 525nm), green band (530nm – 590nm), red band (625nm - 695nm), Near-Infrared band (760nm – 890nm), and panchromatic band (450nm – 745nm) were employed. The sensor characteristic includes 1.5m ortho imagery with an image swath of 60km to maintain a high coverage capability. Mostly, archaeological studies use infrared (760nm – 890nm) and red bands (625nm – 695nm) for spectral analysis [13]. However, some studies used a panchromatic image band to detect the archaeological features. Leveraging screen map area and resolution, SPOT image can compute partial machine-learning-based classifications in a matter of seconds, which is advantageous in developing machine-learning processes. The ability to evaluate the outcomes of fresh training data without having to compute a full-resolution classification of a whole region makes it a crucial benefit over conventional

machine learning methods since it also minimises the number of iterations required to get satisfying results.

Consequently, the study integrated a single type of multispectral imagery data with machine learning-based approaches to detect an archaeological feature in Sungai Batu, Bujang Valley. The different spectral bands of SPOT 7 can reflect soil roughness, texture, dielectric properties, and other ground physical conditions such as compactness. The characteristic compact soil of archaeological features such as mounds that decay clay-based mud bricks formed was assumed to contrast with surrounding desert soil starkly [14]. On the other hand, remote sensing is one of the non-destructive methods used for identifying vegetation stresses related to crop marks stress analysis to determine the buried archaeological remains through colour classification (reflectance properties of plants) [15], [16]. In order to ensure that elements that would yield values similar to mounds in one source were discriminated against in another, the distinct nature of these sensors played a crucial role. Thus, multispectral imaging and machine learning applications were integrated to provide discriminant values for mounded archaeological sites in the area.

**Table 1.** Multispectral SPOT-7 image of Sungai Batu, Kedah, Malaysia.

Sensor	SPOT-7
Characteristics	Image swath of 60-km to maintain a high level of coverage capability
	Resolution with 1.5 m ortho imagery
	Addition of a blue band to get a native natural color image
Spatial resolution	Pan: 1.5m Multispectral: 6m Colour merge: 1.5m
Spectral Bands	<b>Multispectral bands:</b> Blue (0.455 $\mu\text{m}$ – 0.525 $\mu\text{m}$ ), Green (0.530 $\mu\text{m}$ – 0.590 $\mu\text{m}$ ), Red (0.625 $\mu\text{m}$ – 0.695 $\mu\text{m}$ ), Near-Infrared (0.760 $\mu\text{m}$ – 0.890 $\mu\text{m}$ ) <b>Panchromatic band:</b> Panchromatic (0.45 $\mu\text{m}$ – 0.745 $\mu\text{m}$ ),
Swath width	60 km (2 images) 120 km with single-pass mosaic
Geolocation	35 without GCP; < 10 m with Ref3D

### 3. Result and Discussion

This preliminary experiment intends to detect the existing archaeological feature called "*Candi*," using Matching SIFT and ORB descriptors techniques located in the Bujang Valley Archaeology Museum archaeological site. There are three main processing steps to achieve the study's objective, including scale-space, keypoint localisation processes, and feature matching analysis. Meanwhile, histogram-based pixel range analysis is a supported technique that defines the specific group of areas through the pixel range values. Therefore, those images can be used for further comparative analysis in future studies.

#### 3.1 Scale-space

The fact that objects often have multiple scales makes a scale space an attempt to convey this idea on digital images. A function  $L(x,y,\sigma)$  obtained from the convolution of a Gaussian Blurring kernel at

various scales with the input envision is the scale space of an image. The split of scale space into octaves depends on the original image's size, as does the number of octaves. Notably, the image that performed Gaussian Blurring effectively eliminated noise and accentuated the key aspects of the image. These attributes are scale-dependent to maintain consistency and accuracy. Scale-space refers to a set of images with varying scales derived from a single original image. Thus, these blurred images are generated for various scales. Moreover, selecting parameters for Gaussian Blurring involves several factors, such as the size of the kernel and the standard of deviation ( $\sigma$ ) of the Gaussian distribution.

In this study, the size kernel determined for the image is 5x5, generating moderate noise reduction and an appropriate smoothing technique due to high-resolution photos. It will generate several octaves of the original image. Each octave's image size is half the previous one. The odd numbers are preferred because they ensure that there is a central pixel around which the Gaussian distribution is symmetric. Furthermore, the Gaussian Blurring algorithm computes a value for each pixel in the image by considering the values of its adjacent pixels using a specified sigma ( $\sigma$ ) value. The sigma value, the Gaussian function's standard deviation, controls the distribution's spread. A more significant  $\sigma$  results in a broader and smoother Gaussian kernel, leading to more extensive blurring. As a result, a value of  $\sigma=1$  is determined as it helps reduce the noise, simultaneously balancing the noise reduction with preserving significant detail without eliminating many vital information in the image.

As a result, **Figure 4** illustrates the images before (4(a)) and after applying (4(b)-(d)) the Gaussian Blurring. The outcome demonstrates that only the relevant elements are left in the image after eliminating the noise textures and other little details. However, the essential other information is still preserved. The procedures will take the original image and decrease its scale by 50% to generate a new collection of images with varying scales. Subsequently, it will produce blurred versions of each of these new images. In mathematical terms, the process of "blurring" is known as the convolution of the Gaussian operator with the image. The Gaussian blur is implemented by applying a specific mathematical operation to each pixel. The outcome is the image with a blurred effect, as seen in formula (1), while the Gaussian Blur operator is illustrated in formula (2).

$$L(x, y, \sigma) = G(x, y, \sigma) * (I(x, y)) \quad (1)$$

$$G(x, y, \sigma) = \frac{1}{2\pi\sigma^2} e^{-(x^2+y^2)/2\sigma^2} \quad (2)$$

$G$  is the Gaussian Blur operator, and  $I$  is an image. While  $x$  and  $y$  are the location coordinates and  $\sigma$  is the "scale" parameter.



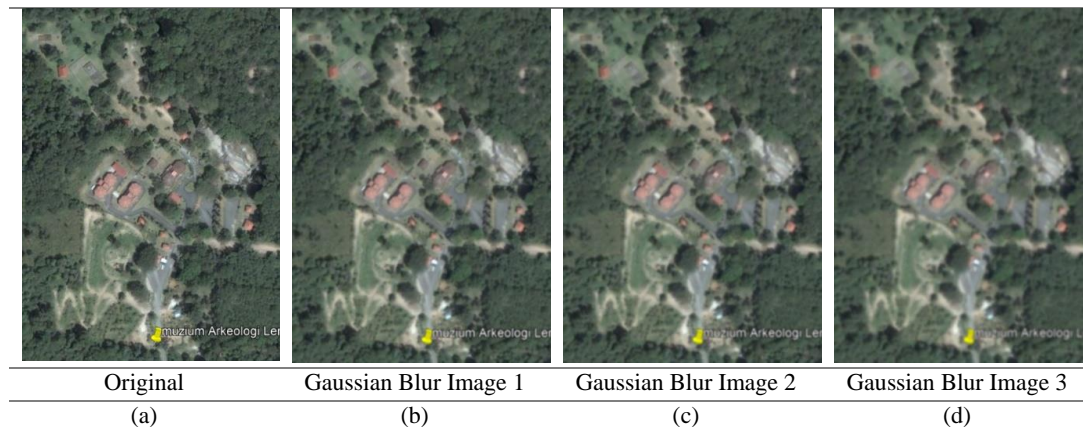


**Figure 4.** (a)Original Images obtained from satellite image SPOT, (b), (c), (d) are images after the filtering processes using the Gaussian Blurring technique.

In the future, the study will strive to improve the characteristics by using the Difference of Gaussians (DoG) methodology. The Difference of Gaussians (DoG) is a technique used in image processing to detect boundaries and extract features. The algorithm involves comparing two images that have undergone Gaussian blurring with different standard deviations.

### 3.2 Keypoint Localisation

Keypoint Localisation completes the SIFT process. **Figures 5(a)** and **5(b)** output are before and after the Gaussian Blurring image filtering. The outcome in **Figure 5(a)** illustrates the image before through "cleaning" edges in the image with lots of keypoint detected, and **Figure 5(b)** demonstrates the keypoint identifying the only significant edges from the image comparison prior to the image filtering processing after the noise was removed.

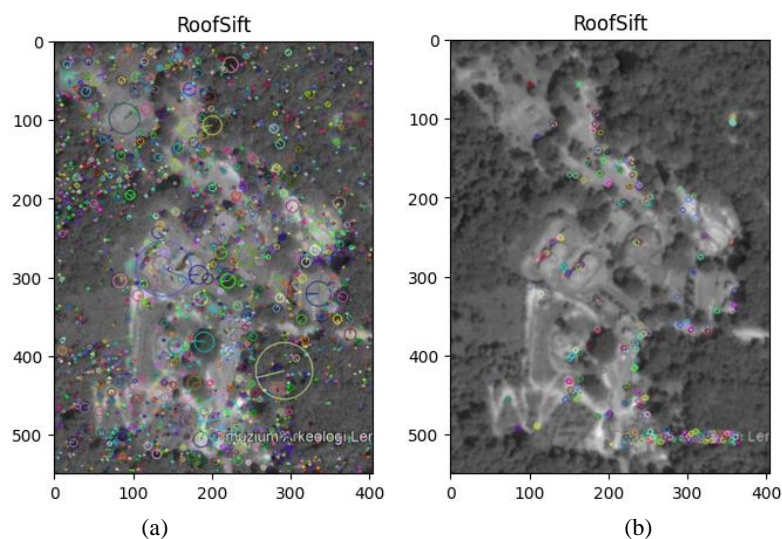
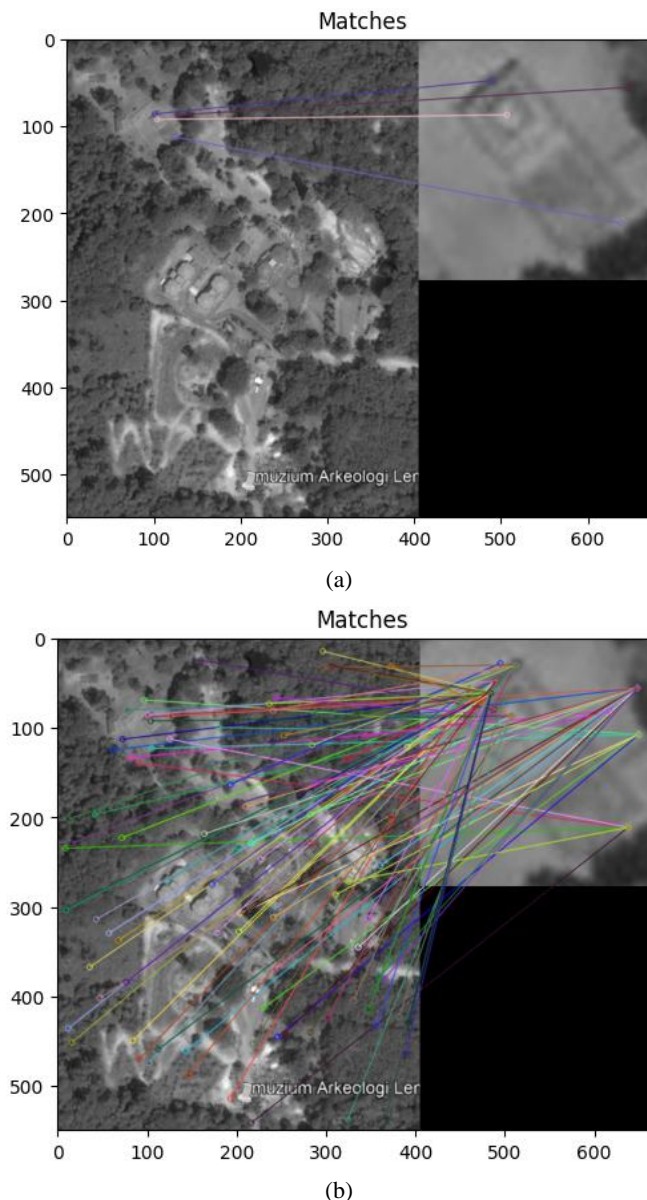


**Figure 5.** (a) Image with keypoint detection with the image before the filtering process (b) image with keypoint detection after the filtering process.

### 3.3 Feature Matching Analysis

In this stage, feature matching is vital to identify and correspond features between two images. Two corresponding images were applied: i) *Candi* and ii) the study area image, consisting of several existing *Candi* with almost the same shape and size as shown. The direct comparing descriptors using the Brute Force Matching method were applied to this image analysis. Besides, the choice of threshold values in the ratio for feature matching is based on the experiment ratio test. Further discussions are explained below.



**Figures 6.** (a) and (b) are comparative images for the feature-matching technique.

Therefore, the results shown in Figure 6 demonstrated that approximately 2373 total matches are defined between both images 6(a) and 6(b). In particular, image 6(a) indicates the ratio test threshold is

$\{m.distance < 0.4 * n.distance\}$ , with the total number of accurate matches being four corrected matches. Meanwhile, precision and recall results are both about 0.0017, or 0.17%. This indicates that just around 0.17% of the matches the algorithm found are accurate. Practically, precision and recall values are crucial metrics for evaluating the performance of an algorithm, especially in the context of classification tasks such as feature detection. This means that the precision-defining proportion of feature detection is correctly identified as a similar object, and the recall value defines the algorithm as successfully detecting a similar object. As a trade-off definition, high precision ensures that detected objects are mostly correct, but some might be missed. High recall ensures that most objects are detected, but some detections might be incorrect.

Nevertheless, after several experiments over ratio test threshold values, it was determined that the best ratio test threshold is  $\{m.distance < 0.8 * n.distance\}$ , which obtained 104 corrected matches, as shown in 6(b). Hence, after the threshold value adjustment to 0.8 from 0.4, the precision improves to approximately 4.38%. This indicates that around 4.38% of all the matches our algorithm discovered are accurate, and the matches are correct since they pass the ratio test. Subsequently, the ratio of correct matches to the total number of matches after applying the ratio test- the matching score is 1.0. This indicates that all the matches that passed the ratio test are correct. This matching score remains at 1.0, indicating that all the matches that pass the adjusted ratio test threshold are correct for image 6(b). It is suggested that the threshold value of 0.4 might have been too strict, discarding many correct matches. However, if the value is below 0.4, the value is invalid, and no matching is determined. Thus, adjusting the threshold to 0.8 has improved the overall performance of the keypoint matching technique.

### *3.4 Histogram-Based – Pixel Range Analysis*

Image identification utilising histogram-based analysis entails examining the pixel values inside an image to uncover this study's patterns and features of interest. In this study, analysis of the histogram graph of an image is conducted to discover peaks (minimum and maximum value) that correspond to distinct features or characteristics based on the distribution of pixel intensities. Thus, from the histogram analysis, one can identify patterns or irregularities that may not be readily observable from a self-interpretation of the image. Instead, this technique is one of the possible approaches depending on intricate algorithms or deep learning models, which concentrate on basic comparisons of pixel values within defined ranges. Histogram-based methods are typically efficient in terms of processing and straightforward to implement, making them well-suited for real-time applications or scenarios with limited computational resources. Nevertheless, these methods may lack the durability and precision of more advanced techniques, particularly when confronted with intricate or distorted images.

Therefore, the graph below illustrates the minimum and maximum of the image in pixel values in the histogram graph, as shown in Figure 7. Technically, the RGB images were converted to greyscale images, and later, four groups of minimum and maximum values of pixel ranges were tested. Later, the graph was plotted with the X-axis pixel values and the Y-axis frequency values. As illustrated in Figure 8 (a), the testing of pixel value ranges was selected based on minimum to maximum pixel value in two parts of the division. First, minimum and maximum values were chosen between the range 40-75. The second division is between 110 -140 at minimum and maximum values. The result shows that most of the range of pixel values between 40-75 were plotted in the vegetation area in the study area. Meanwhile, the range of pixels between 110-140 recognised the build-up area, including archaeological monuments. Moreover, the range of pixels between 120-140 classes is more detailed in terms of the build-up area, including archaeological features, and the range of pixels between 130-140 specified more detailed build-up area, including archaeological features eliminated vegetation pixels.

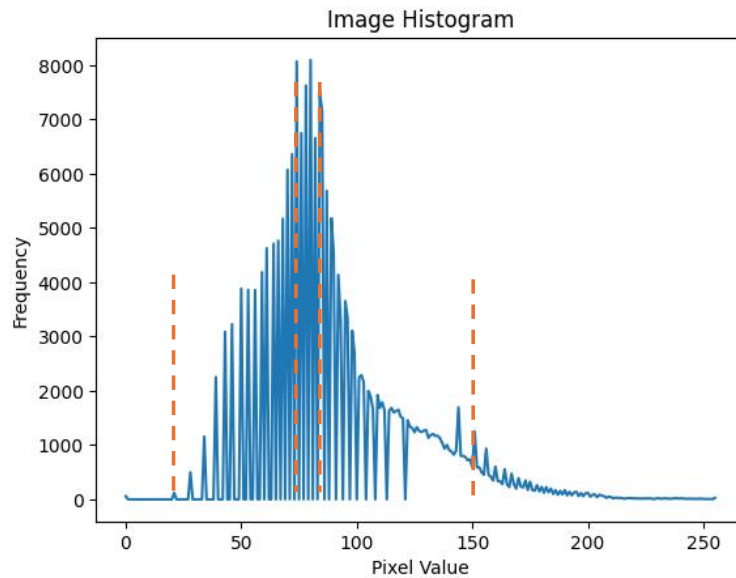
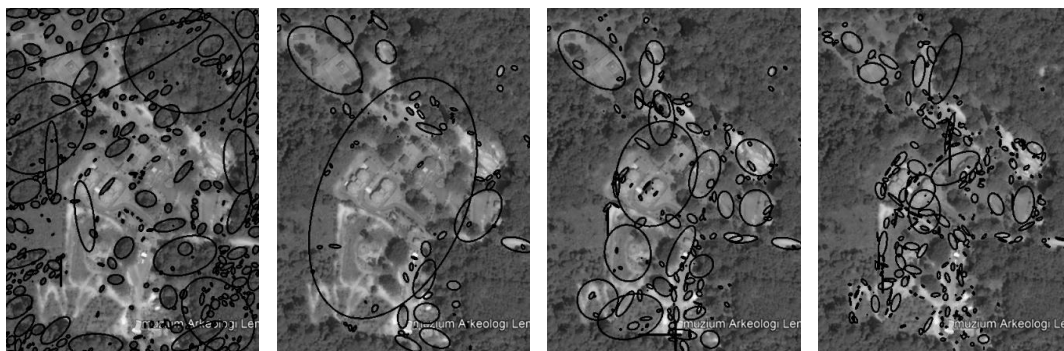


**Figure 7.** The histogram graph has minimum and maximum pixel values against the frequency of the image

Location at Bujang Valley near to Jerai Mount



The range of pixels between 40-75 defined the area of vegetation.

(a)

The range of pixels between 110-140 defined the build-up area, including archaeological features.

(b)

The range of pixels between 120-140 defined the build-up area, including archaeological features.

(c)

The range of pixels between 130-140 defined the build-up area, including archaeological features.

(d)

**Figure 8.** (a)-(d) Image detection using the pixel-range-based technique to identify the type of features in the study area through maximum and minimum pixel values.

#### 4. Conclusion

In conclusion, integrating Artificial Intelligence, mainly through applying Scale-Invariant Feature Transform algorithms, has significantly impacted archaeological feature detection and image interpretation. By leveraging high-resolution multispectral satellite imagery, this preliminary study focuses on techniques to detect potential hidden archaeological features in Bujang Valley, Kedah, Malaysia. The expected outcome is to provide valuable insights into the extent and distribution of archaeological features in the targeted region, contributing significantly to our understanding of the area's archaeological landscape and history by using a Bag of Visual Words (BoVW) model- SIFT and ORB algorithms consisting of Gaussian Blurring, Keypoint Localization, and Keypoint Matching processes. This technique can accurately predict the hidden archaeological features within the generated maps. Finally, utilising AI and advanced algorithms enhances the efficiency and reliability of large-scale archaeological mapping and presents a promising avenue for uncovering previously unknown archaeological remnants. For future works, this study will continue experimenting with several feature-extracting algorithms to compare with the SIFT algorithm, which matching methods will achieve better performance.

#### Acknowledgements

The Ministry of Higher Education Malaysia financially supported this study under the Fundamental Research Grant Scheme FRGS/1/2022/TK07/UTM/02/52. The authors also would like to thank the Geophysics Unit of the University of Sciences Malaysia (USM), the Centre of Global Archaeology Research, USM, and Mr. Sheyh Sahibul Karamah Masnan for their cooperation. Also, the Municipality of Department Heritage Malaysia and Malaysia Remote Sensing Agency (MYSA) provided satellite information data for this study.

#### References

- [1] A. Argyrou, A. and Agapiou, "Review of Artificial Intelligence and Remote Sensing for Archaeological Research", *A Remote Sensing Journal, MPDO*, vol. 23, 2022.
- [2] L. Magnini and C. Bettineschi, "Theory And Practice For An Object-Based Approach In Archaeological Remote Sensing," *Journal Archaeological Science.*, vol. 107, no. May, pp. 10–22, 2019.
- [3] M. Soroush, A. Mehrtash, E. Khazraee, and J.Ur, "Deep Learning In Archaeological Remote Sensing: Automated Qanat Detection In The Kurdistan Region of Iraq.," *A Remote Sensing*, 2020.
- [4] S. Sharafi, S. Fouladvand, I. Simpson, and J. Alvarez, "Application Of Pattern Recognition In The Detection Of Buried Archaeological Sites Based On Analysing Environmental Variables, Khorramabad Plain, West Iran," *Journal of. Archaeological Science Report*, 206–215, 2016.
- [5] L. Casini, M. Rocchetti, G. Delnevo, N. Marchetti, and V. Orrù, "The Barrier Of Meaning In Archaeological Data Science," *In Proceedings of the SCIFI-IT' 2020—4th Annual Science Fiction Prototyping Conference, Ghent, Belgium*, 61–65, 2020.
- [6] M. Saidin and S. Shahidan, "Engaging Archaeology Through Performing Arts: Prospect And Challenges In Malaysia," *Wacana Seni Journal of Arts Discourse* 18, 1–9, 2019.
- [7] T. Adi, "Archaeology in Peninsular Malaysia: Past, Present and Future," *JASTOR*, 1987.
- [8] NH. Rahman, "Recent Archaeological Discoveries In Sungai Mas, Kuala Muda, Kedah," *Journal of the Malaysian Branch of the Royal Asiatic Society*, 73–80, 1993.
- [9] T.T. Khoo, "Geomorphological Evolution of The Estuary Area And Its Impact On The Early State of Kedah, Northwest Peninsular Malaysia," *JASTOR*, 9547, 1996
- [10] S. Chia, and B.W. Andaya, "Bujang Valley and Early Civilisations in Southeast Asia," *Kuala Lumpur: Department of National Heritage of Malaysia*.

- [11] M. Jacq-Hergoualc'h, "La Civilisation de Ports-entrepots du Sud Kedah (Malaysia)" Ve-XIVe Siecle.Paris I 'Harmattan, 1992.
- [12] J.S. Allen, "Trade Transportation and Tributaries: Exchange, Agriculture, and Settlement Distribution in Early Historic Period Kedah, Malaysia," (Doctoral Dissertation). Malaysia: Hawaii: University of Hawaii, 1988
- [13] G. Verhoeven & M. Doneus, "Balancing on the Borderline – A Low-Cost Approach To Visualise The Red-Edge Shift For The Benefit of Aerial Archaeology,". 267–278, 2011.
- [14] R. H.-N. Fenger-Nielsen, "Footprints From The Past: The Influence Of Past Human Activities On Vegetation And Soil Across Five Archaeological Sites In Greenland," *Journal of Science of the Total Environment*, 654, 895–905, 2011.
- [15] A. Agapiou, D.G. Hadjimitsis, A. Georgopoulos, A. Sarris & D.D. Alexakis, D.D., "Towards An Archaeological Index: Identification Of The Spectral Regions Of Stress Vegetation Due To Buried Archaeological Remains," *Lect. Notes Comput. Sci. (including Subser. Lect. Notes Artif. Intell. Lect. Notes Bioinformatics)*, vol. 7616 LNCS, 129–138, 2012.
- [16] A. Agapiou, D.G. Hadjimitsis, A. Georgopoulos, A. Sarris & D.D. Alexakis, D.D., "The Optimum Temporal And Spectral Window For Monitoring Crop Marks Over Archaeological Remains In The Mediterranean Region," *Journal Archaeological Science*, vol. 40, no. 3, 1479–1492, 2013.